EXTREME ULTRAVIOLET LIGHT POLARIMETRY

By

Nathan Heilmann

A senior thesis submitted to the faculty of

Brigham Young University – Idaho

in partial fulfillment of the requirements for the degree of

Bachelor of Science

Department of Physics

Brigham Young University - Idaho

March 2008

BRIGHAM YOUNG UNIVERSITY – IDAHO

DEPARTMENT APPROVAL

of a senior thesis submitted by

Nathan Heilmann

This thesis has been reviewed by the research committee, senior thesis coordinator, and department chair and has been found to be satisfactory.

Date	Todd Lines, Advisor
Date	Ryan Nielson, Senior Thesis Coordinator
Date	Evan Hansen, Committee Member
Date	Steven Turcotte, Department Chair

ABSTRACT

EXTREME ULTRAVIOLET LIGHT POLARIMETRY

Nathan Heilmann

Department of Physics

Bachelor of Science

Using Extreme Ultraviolet light from high harmonic generation from an 800 nm laser source, we can determine the index of refraction of a sample material. By taking the ratio of the reflectance of p and s polarizations, we can use least-squares fitting method the calculate index of refraction from the curve. The thickness of a thin layer can also be calculated if the chosen sample is less than 16 nm thick. By modeling the reflectance curve of EUV off of silicone dioxide, it has been determined that for this material that if the thin layer is greater than 16 nm that it is essentially infinite in thickness. This interferometer has been tested using two samples of silicone dioxide, one 27 nm thick and the other is 2 nm thick.

ACKNOWLEDGMENTS

I would like to thank Justin Peatross, Nichole Brimhall, and Nicholas Herrick for helping me during my Internship and understanding the research. I would also like to thank everyone at BYU – Idaho for helping me write my paper and offer support.

I also thank the National Science Foundation (Grant #PHY-0457316) for funding the Research.

CONTENTS

ABSTRACT v
ACKNOWLEDGMENTS vii
CONTENTS ix
LIST OF FIGURES xi
CHAPTER 1 – INTRODUCTION AND BACKGROUND 1
1.1 Why Study EUV 1
1.2 High Harmonic Generation 2
1.3 Past Studies 5
CHAPTER 2 – SETUP AND EUV GENERATION 7
2.1 EUV Generation 7
2.1.1 *Laser Setup* 7
2.1.2 *Gas Chambers* 8
2.1.3 *Test Chamber* 9
2.2 Necessary Equipment 11
2.3 Other Methods 11
CHAPTER 3 – PROCEDURE AND DATA ANALYSIS 13
3.1 Computer Simulation 13
3.2 Preparation and Procedures 15
3.3 Reflection of EUV 17
3.3.1 *Sample Material* 17
3.3.2 *Sample Thickness* 17
3.4 Analyzing Data 18
CHAPTER 4 CONCLUSION 21
4.1 Conclusion 21
4.2 Ideas for New Study 21
REFERENCES 23
Appendix: Matlab Code 24

LIST OF FIGURES

Figure 1.1 – The Electromagnetic spectrum. [8] EUV light is between UV light and X-rays 1

Figure 1.2 – The Fringe pattern generated on a phosphorous screen by high-harmonics orders, the number above the fringes correspond to the harmonic order that generated it. The white patch n the middle of the screen results when the beam is too strong and the detector is saturated. [3] 3

Figure 1.4 – The Setup of the original EUV prototype at BYU. [3] 6

Figure 2.1 – A depiction of the p and s polarizations. [5] 7

Figure 2.2 – The first two vacuum chambers, the first is the generating cell where the EUV light is generated.... 9

Figure 3.1 – Curves of varying thicknesses generated in Matlab using a wavelength of 29.6 nm, and index N=.9109+i*.0853 (Index given by the Center for X-Ray Optics [9]). 13

Figure 3.2 – Curves of varying index of refraction generated in Matlab using a wavelength of 29.6 nm and thickness of 5 nm (The top two graphs) and 40 nm (The bottom two graphs), centered around the index of refraction N=.9109+i*.0853 (Index given by the Center for X-Ray Optics [9]). 14

Figure 3.3 – The procedural steps for aligning the Polarimeter [3] 16

Figure 3.5 – data for Absolute Rp and Rs measurements, compared with measurements from CXRO............... 19

Figure 3.6 – data for Rp/Rs measurements off the 27 nm sample, compared with CXRO................................. 20

CHAPTER 1 – INTRODUCTION AND BACKGROUND

1.1 Why Study EUV

Extreme Ultraviolet light (EUV) has a variety of uses and can be effective in many fields such as lithography, space-based astronomy, and microscopy; since EUV has shorter wavelengths than ultraviolet light (UV), ranging from 1 nm to 100 nm, experiments which will need the use of shorter wavelength can be modified to use EUV. Because EUV light is easily absorbed by lenses, which are used to redirect and focus UV light, a system of mirrors can be used in place of the lenses. The shorter wavelengths of EUV also have a higher energy, which over time can damage the surface of a mirror; similar experiments can also be performed with x-rays, which have a shorter wavelength then EUV, but since x-rays are more powerful they damage the sample surface faster than EUV, making it more logical to focus on the studies of EUV.

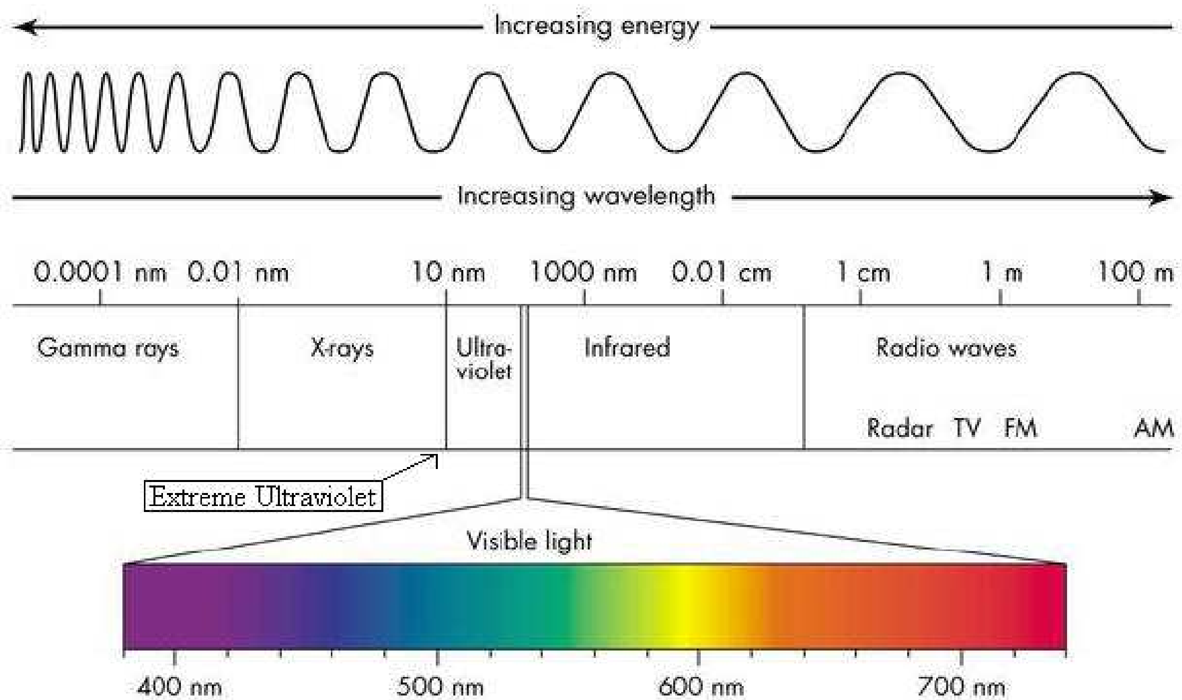

Figure 1.1 – The Electromagnetic spectrum. [8] EUV light is between UV light and X-rays

Since the index of refraction can shift depending on the wavelength of the light that is interacting with it, the index of refraction is not always known for these shorter wavelengths. Until the index of refraction can be determined, the effectiveness of a material as a reflector for EUV is also unknown. The index of refraction can be calculated by measuring the EUV reflectance off of a selected material. There are multiple sources for generating EUV, a researcher could travel to a Synchrotron which would have a very bright and reliable beam, or they could use a plasma source which is smaller and more portable but very restrictive on the available wavelengths. At BYU, I did my research with Graduate Student N. Brimhall, under the guidance of Professor J. Peatross; we used laser generated high harmonic orders to generate EUV in a gas chamber. Laser generated EUV offers a selectable polarization, and a range of wavelengths. This source is portable, small, and located on the BYU campus, but the accuracy of the measurements is unknown.

Through adaptations of past BYU experiments of laser generated high harmonic orders in the extreme ultraviolet wavelength range, the accuracy of the system can be determined through comparison of calculated index of refraction from other EUV sources against the calculated results from laser generation. By measuring the reflectance of polarized EUV off of a sample material, we can use the resulting data to calculate the index of refraction of the sample. By first measuring the reflectance of a material which is commonly used and already has an accepted index of refraction, our experimental results should match the materials accepted value which has been determined and tested by the other sources for EUV. [3]

1.2 High Harmonic Generation

At BYU, we used an 800 nm infrared laser with ~10 mJ of energy in 30 fs pulses. The high-intensity beam is directed through a converging lens into the first chamber, which has been pumped to below 1 torr and then filled with a chosen gas. (See section 2.1.2) The harmonics are then generated

within this gas, with the wavelengths produced dependent upon the type. The harmonics, along with some of the residual infrared laser, exit the generating gas through a thin layer of molybdenum foil at the focus point of the laser. To keep the opening as small as possible, the laser itself is used to burn a hole in the foil, which has the advantage of automatic alignment for the opening into the secondary vacuum chamber.

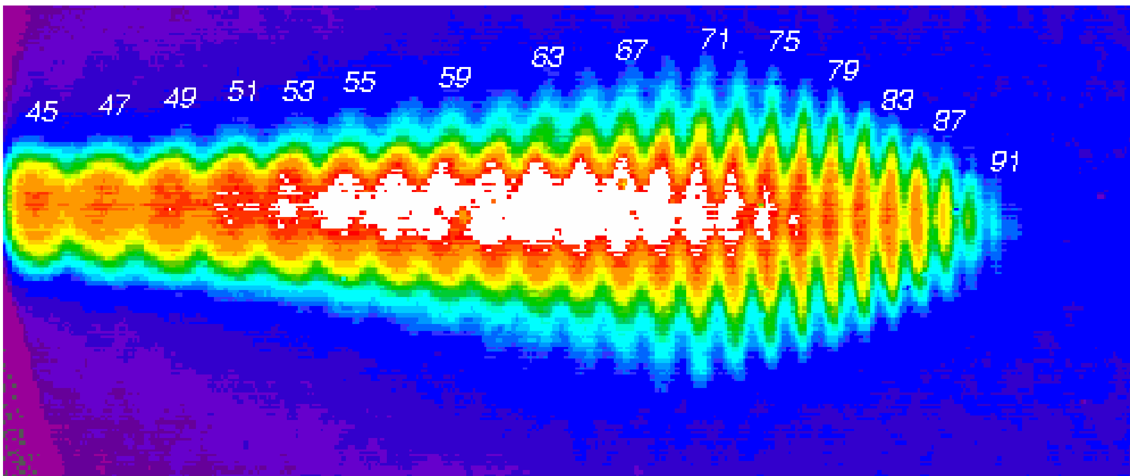

Figure 1.2 – The Fringe pattern generated on a phosphorous screen by high-harmonics orders, the number above the fringes correspond to the harmonic order that generated it. The white patch in the middle of the screen results when the beam is too strong and the detector is saturated. [3]

The harmonic orders can be determined using the incident angle and the resulting angles of the grating, and also by tracking the shifting fringes as the angle is shifted for measuring. For simplicity, an aluminum filter is used to quickly determine the harmonic order of the fringes. (See section 2.1.3) The wavelength of these harmonic orders can be calculated using Eq. (1). [7]

$$\lambda_q = \frac{\lambda_i}{q} \tag{1}$$

In this equation λ_q is the harmonic wavelength, λ_i is the incident wavelength, and q is the harmonic

order. Because a gas is used to make the harmonics, only the odd harmonics are able to be produced. In order for the even harmonics to be generated you would need a crystal structure of atoms instead of a free flowing gas. The secondary vacuum chamber is either kept at a base of .03 torr or pumped down to the base and then has another gas pumped back in at a stable pressure, chosen between .05-2 torr. This secondary chamber is used for absorption tests as well as to dampen the harmonic signal to avoid saturating the detector with too bright of a signal. Saturation of the detector is observed in figure 1.2, the white patch in the middle is the saturation, where the strength of the beams reflectance cannot be measured properly. At the other end of the secondary chamber is another small opening which opens into the main vacuum chamber where the EUV is reflected off of the sample into a small inner chamber to be measured.

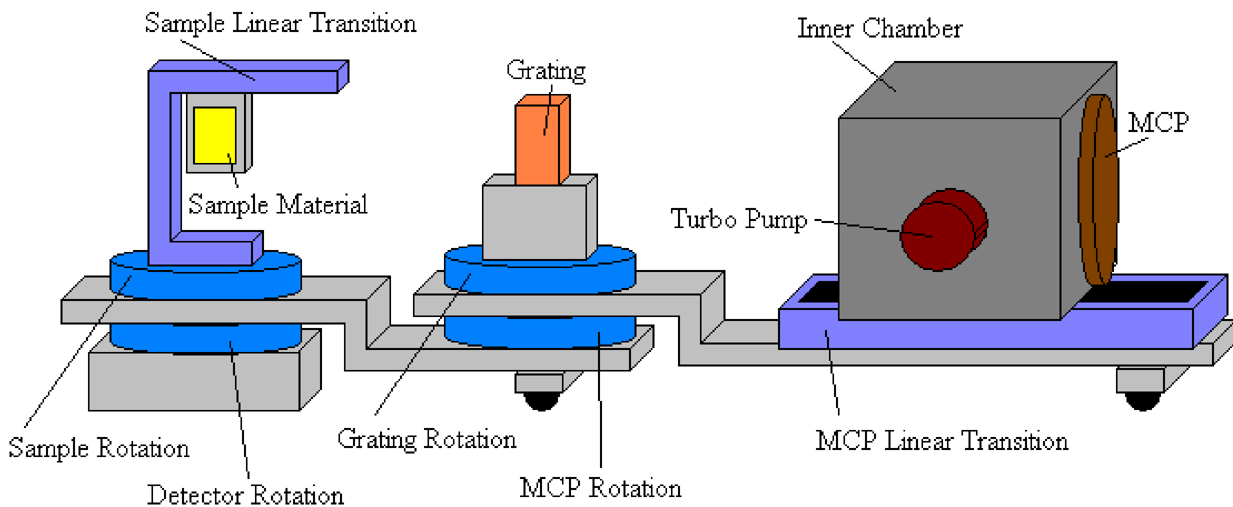

Figure 1.3 – The Internal Setup of the main Vacuum Chamber at BYU.

In the main chamber is a system of arms and motors which allow the angle of incidence to be altered without having to open the chamber, as seen in figure 1.3. First the EUV beam is directed at the reflection sample, and then a grating is used to separate the wavelengths of the harmonic orders. After the grating has split the harmonics, the split beam enters the small inner vacuum chamber located

inside the main chamber. This inner chamber is kept at a lower pressure of at least 10E-6 torr by its own vacuum pump. This small chamber houses a high voltage micro-channel plate (MCP) coupled to the phosphorus screen, which is illuminated by the separate fringes of the impacting EUV beam, and then recorded by a camera, as observed in figure 1.2. (See section 2.1.3) [3]

1.3 Past Studies

A former graduate student at BYU had previously constructed a simple prototype of vacuum chambers which had the ability of selecting the polarization for reflection measurements. Although this prototype was capable of measuring EUV light, it could only operate at a fixed angle. The prototype used a half wave plate to polarize the incident beam with argon gas in the primary chamber to produce the high harmonic orders. By using the half wave plate, the polarization could be easily rotated, allowing for quick comparison measurements. The harmonics would then be reflected twice, first off the sample material and then at an opposing angle with a grating, which would separate the range of wavelengths. After the wavelengths are separated by the grating, the beam impinges upon a phosphorus screen, coupled with a micro-channel plate. By using the grating, multiple wavelengths are able to be measured simultaneously, which also shortens the time it takes to perform measurements. The setup of the prototype can be seen in figure 1.4.

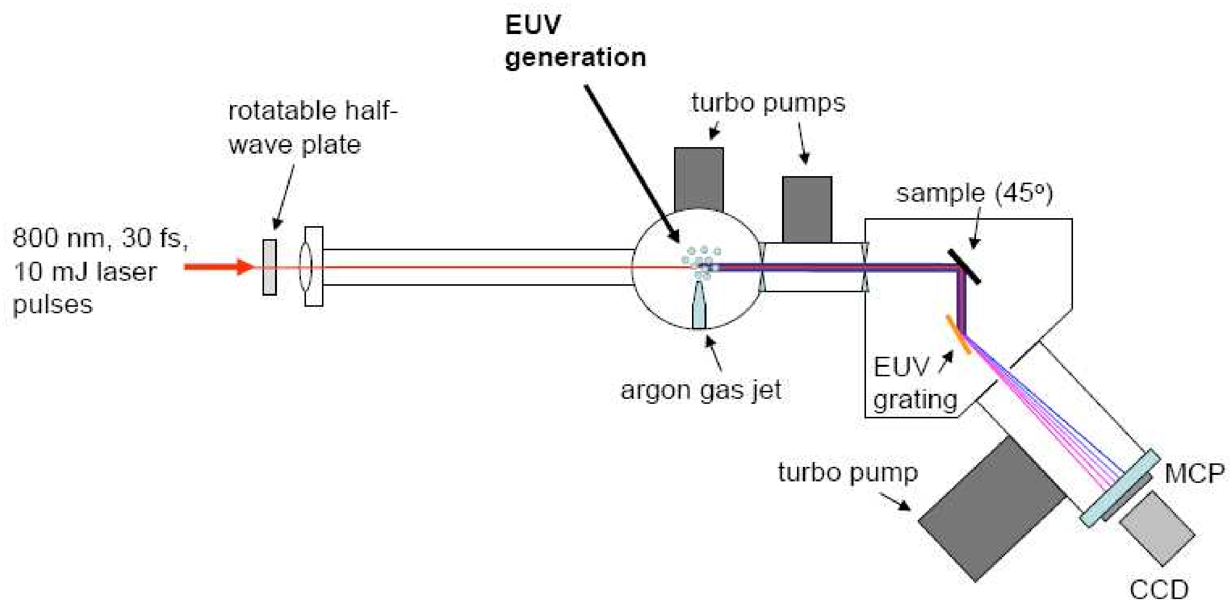

Figure 1.4 – The Setup of the original EUV prototype at BYU. [3]

The primary drawback of the prototype is the fixed angle of the sample material at 45 degrees, only one point in a range of angles, where measuring more angles would give the system a higher accuracy. Also with the light beam being reflected twice before measuring, the sample could not be removed for an incident measurement. Although the angle remained fixed, the incident measurement was partially resolved by placing a "reference" substance partially in the pathway of the beam along with the sample. [3]

CHAPTER 2 – SETUP AND EUV GENERATION

2.1 EUV Generation

2.1.1 *Laser Setup*

High-harmonics generated by laser are an excellent source for a range of focused and polarized EUV wavelengths. The ranges of wavelengths available at BYU are 8-62 nm, appearing in a fringe pattern on the sensor as shown in figure 1.2. As mentioned briefly in section 1.2, the system used to generate these harmonics is a 10 mJ laser with a pulse rate of 10 Hz, being amplified by an array of titanium-sapphire crystals. With pulses of only 30 fs, this laser has a wavelength near 800 nm, which is in the infra-red part of the electromagnetic spectrum (See figure 1.1). As with the prototype, a half-wave plate is used to polarize the laser just before entering the first vacuum Chamber. This half-wave plate is also mounted with a rotational motor which gives us the ability to rotate it quickly and accurately, allowing a quick change between p-polarization and s-polarization.

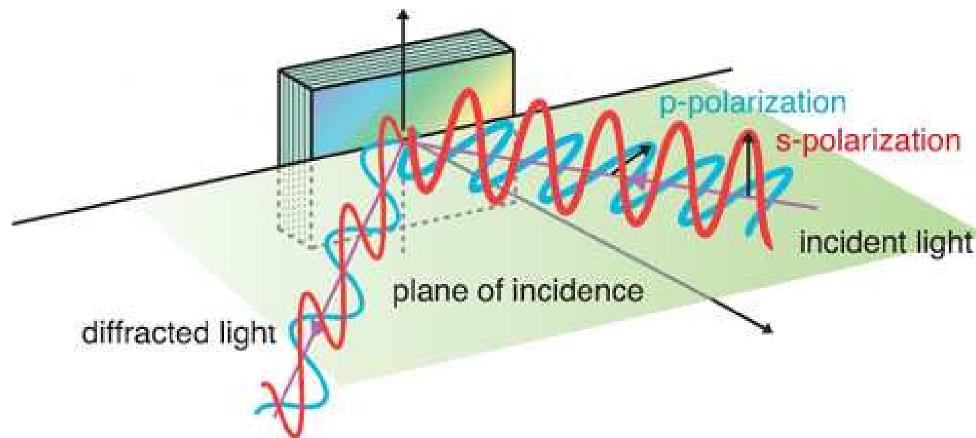

Figure 2.1 – A depiction of the p and s polarizations. [5]

The terms of p and s polarizations describe the orientation of the light with respect to the sample material it is being reflected, where p-polarization means that the light is polarized perpendicular to the surface, and s-polarized is parallel to the surface. The laser is then projected into the first vacuum

chamber through a 100 cm focal length lens, the length of the first chamber, with the focal point of the lens at the molybdenum foil.

2.1.2 *Gas Chambers*

The laser is directed into the first vacuum chamber, or generating cell, that is used to maintain a certain pressure of gas in which the harmonic orders are to be generated. Because each gas has a different density, atomic mass, and number of electrons, the pressure selected depends on the gas that is used; 100 torr if the gas is Helium, 60 torr for Neon, and 12 torr for Argon. The harmonics are created when the incident laser beam focuses at the end of the generating gas cell with an intensity of approximately 10^{15} W/cm^2. The pulses of the laser cause nonlinear responses in the atoms of the gas, which causes harmonics of EUV light to be generated within the gas. The EUV harmonics being created propagate along the original pathway of the incident infra-red laser, along with the residual incident laser that doesn't get absorbed by the gas. The EUV light also maintains the same polarization, giving us choice of the polarization of the beam, also allowing the polarizer to be placed outside of the vacuum chambers. A diagram of the first chamber is depicted in figure 2.2 shown below.

At the end of this chamber is a glass tube, ~4 inches long with ~1 inch diameter, protruding into the next chamber, which is attached as a cap for the first chamber. This glass tube is easily removed, allowing for molybdenum foil to be glued to one end and inserted back into the chamber. Since the location of the greatest EUV generation is near the focus point of the incident beam, to maximize the generation of the harmonics, the glass tube is adjusted until the foil is placed precisely at the focus point. This adjustment for the beam to propagate through the foil immediately after generating EUV is to maintain the strength of the beam, since the EUV beam can be reabsorbed by excess gas. The foil is replaced after every run, to minimize the number of gas leaks into the second chamber, making it is very difficult to ever measure the precise spot for the pin-hole to be located. As mentioned in the

introduction, the infrared beam is used to drill, or burn, a hole in the correct position every time the foil is replaced.

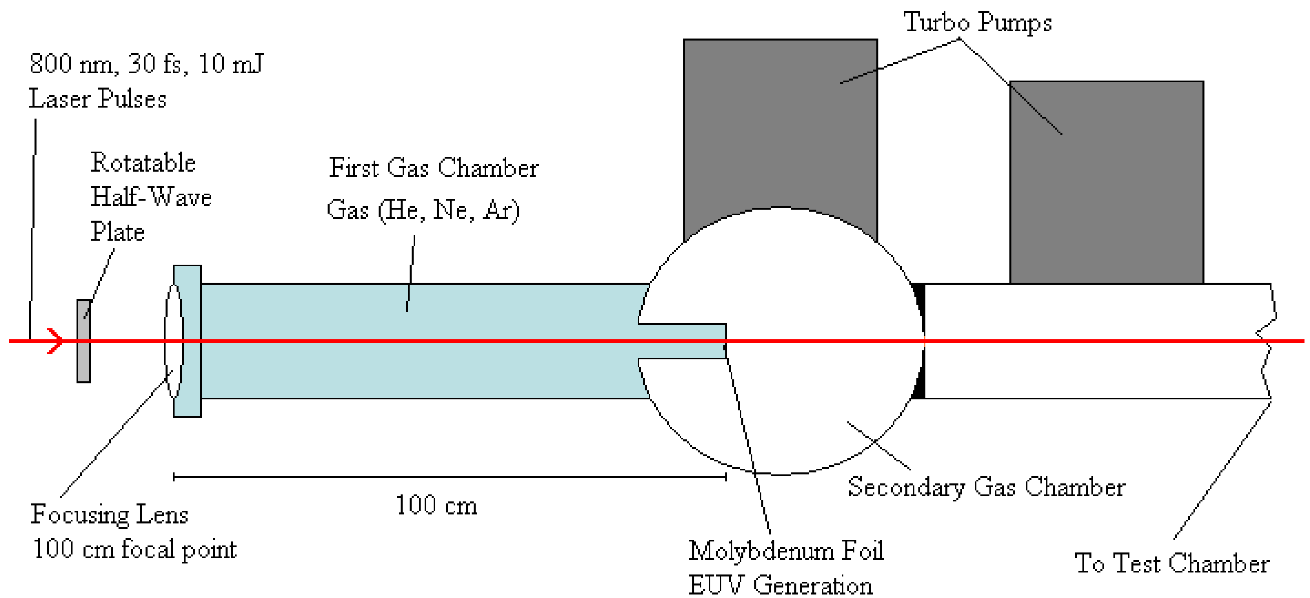

Figure 2.2 – The first two vacuum chambers, the first is the generating cell where the EUV light is generated.

The secondary chamber is at a lower pressure than the first, preferably a very low vacuum. But due to leaks in the system, including the hole in the molybdenum foil, the second chamber is maintained in the range between .05 and 2 torr. The lower pressure of the secondary chamber is preferred since the now generated high-harmonic orders are absorbed very easily, even by the generating gas. This secondary chamber also has the option for adding gas for a higher pressure, which will be described later in section 3.3. The beam then continues into another small opening opposite the foil, into a large vacuum chamber which houses the sample and detector.

2.1.3 *Test Chamber*

After entering the large test chamber, there is a small motor with an aluminum filter on it which can be placed in the path of the beam, as depicted in figure 2.3. This filter blocks wavelengths over the

47th harmonic, allowing us to start at the unblocked fringe and count out the harmonic orders instead of calculating them from the angles. After determining the 47th harmonic order, the filter can then be removed, allowing unhindered measurements to be taken.

The pressure of this larger chamber is kept as low as possible by a large turbo-molecular pump. Unlike the fixed angle from the prototype, the sample, grating, and the MCP are positioned on movable arms. As depicted in figures 1.3 and 2.3, there are dual rotation motors which allow the arms to move, changing the angle of incidence, and can rotate the sample and grating, which allow for small corrections. There are two other motors, one to adjust the distance of the chamber housing the MCP from the grating, and another which can move the sample out of the path of the beam, see section 3.2.

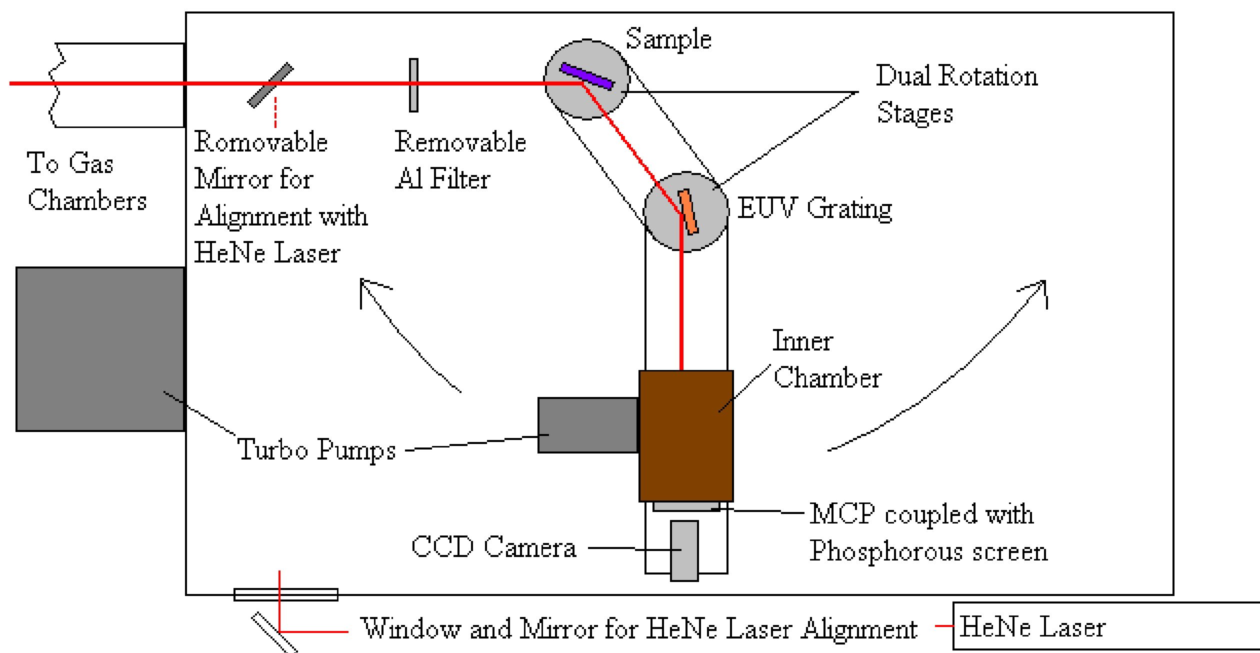

Figure 2.3 – A diagram of the Test Chamber at BYU

When the system is aligned for measurements, the sample reflects the beam onto a focusing tungsten-coated EUV grating (The focal point of the grating is far beyond the MCP and phosphorous screen). The grating is used to separate and focus the wavelengths at slightly different angles into a

small vacuum chamber which houses the MCP. This small chamber holds the MCP, coupled with a phosphor screen, at a pressure of at least 10E-6 torr. This smaller chamber is maintained at this pressure by its own turbo molecular pump inside the large chamber. As the separated EUV light strikes the phosphor screen it creates luminescence which is recorded by a CCD (charge coupled device) camera. This data, relayed to the computer, is then analyzed and used to determine the reflectance, which is described more in section 3.4.

2.2 Necessary Equipment

With a majority of the system and equipment already owned and assembled at BYU, there are only a few materials and pieces of equipment required for this experiment. The main items needed are a supply of molybdenum foil, torr-seal, and a steady flow of water. The use of the foil was described in section 2.1.2, and the torr-seal is an epoxy which is used to attach the foil to the glass tube between the primary and secondary gas chambers, and the water is used as a coolant for the laser and vacuum pumps. All of the necessary equipment for the maintenance/repair of the chambers and laser when needed, is already available and is located on the BYU campus.

2.3 Other Methods

Multiple ways of generating EUV exist, which can be used to test reflectance. Using a Synchrotron can be a very steady and strong source, but it is large, expensive, and has fixed polarization. Another way is to use a plasma source, which is smaller but offers a lower number of wavelengths and is not polarized. BYU has two methods of EUV generation on campus, the first being laser generated high-harmonics, and the other is through a plasma source. The plasma source is fairly reliable, but offers only a few fixed wavelengths and has a much weaker signal than the other two sources. [3]

Experiments at BYU have also been done at a synchrotron, but it requires the assembly of all necessary equipment and traveling to one of the labs housing a synchrotron. A synchrotron is a very large facility, which houses a system of particle accelerators arranged in a very large circle. This system of accelerators will propel an electron in this loop at very high speeds, adding more energy to the electron every time it passes an accelerator. As the electron slows, it radiates the excess energy through emission, a projection of photons through openings arranged along the outer edge of the loop. These electron emissions have a high intensity and wide range of wavelengths, allowing for multiple experiments and a reliable source.

Although a synchrotron is very reliable, and offers a very bright incident source, it has a few disadvantages. The produced beam of light is not completely polarized in one direction, but has a fixed 90% s-polarization and 10% p-polarization. The synchrotron is also a hundred-million-dollar instrument with a permanent staff of hundreds of people. [1] The laser generated high-harmonics is a small fraction of the cost and can be operated by a single person, and would be beneficial if able to produce the same results as a synchrotron.

CHAPTER 3 – PROCEDURE AND DATA ANALYSIS

3.1 Computer Simulation

Before and during the experiment, I used matlab [6] to model the reflectance of the polarization ratios. (See Appendix A) Through these models of reflectance, I would vary the thickness, angle, or even the index of refraction to observe how the data curve would react to the changing variables. Although the thickness and index of refraction for a sample would be constant; any unknown variables would be calculated more accurately if a small change would shift the data, as depicted by the simulated model shown in figures 3.1 and 3.2. Even though actual measurements would only have the angles range between 5 and 45 degrees, I modeled the range from 0-90 degrees to keep in mind any unpredicted results at angles greater than 45 degrees. A majority of the variance in the expected data curve of measurements are predicted to happen before reaching the effective Brewster's angle.

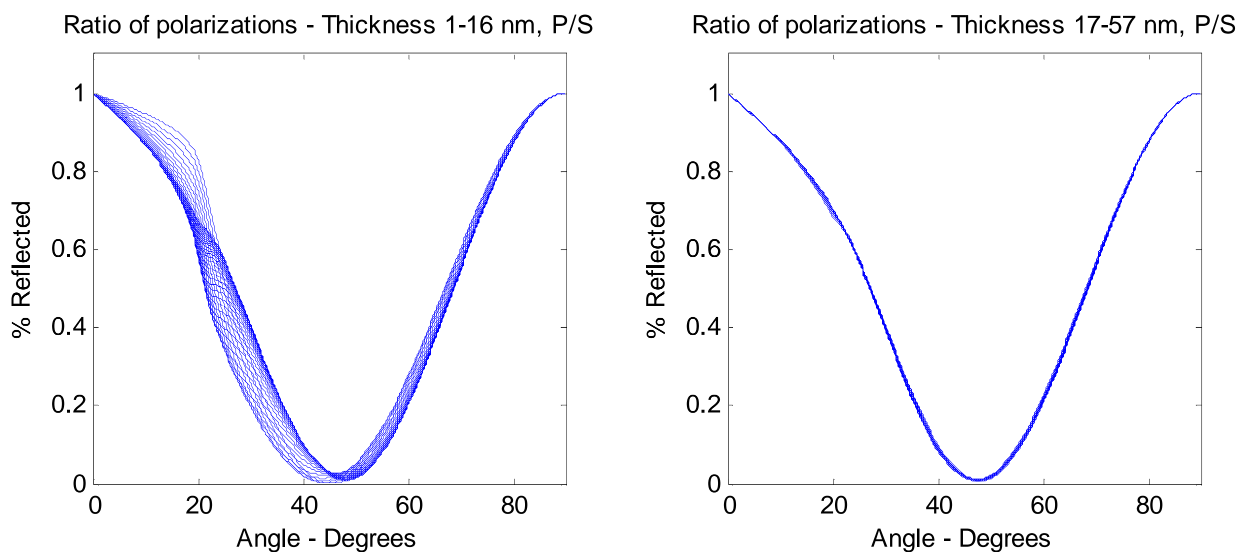

Figure 3.1 – Curves of varying thicknesses generated in Matlab using a wavelength of 29.6 nm, and index N=.9109+i*.0853 (Index given by the Center for X-Ray Optics [9]).

Varied thickness is depicted in figure 3.1. The model shows that samples of 16 nm or less would be more effective in producing an acceptable reflectance curve for calculating the index of refraction.

Where any thickness 17 nm or greater will have a very small shift in the data, still able to calculate the index of refraction but any calculation of thickness will not work. (See section 3.3) When shifting the index of refraction, I would shift both parts (where the index is N=n+i*κ, n is the real part, and kappa the imaginary) at different thicknesses, as depicted in figure 3.2. The graphs also show that the index of refraction can be more accurately calculated when using a sample less than 16 nm.

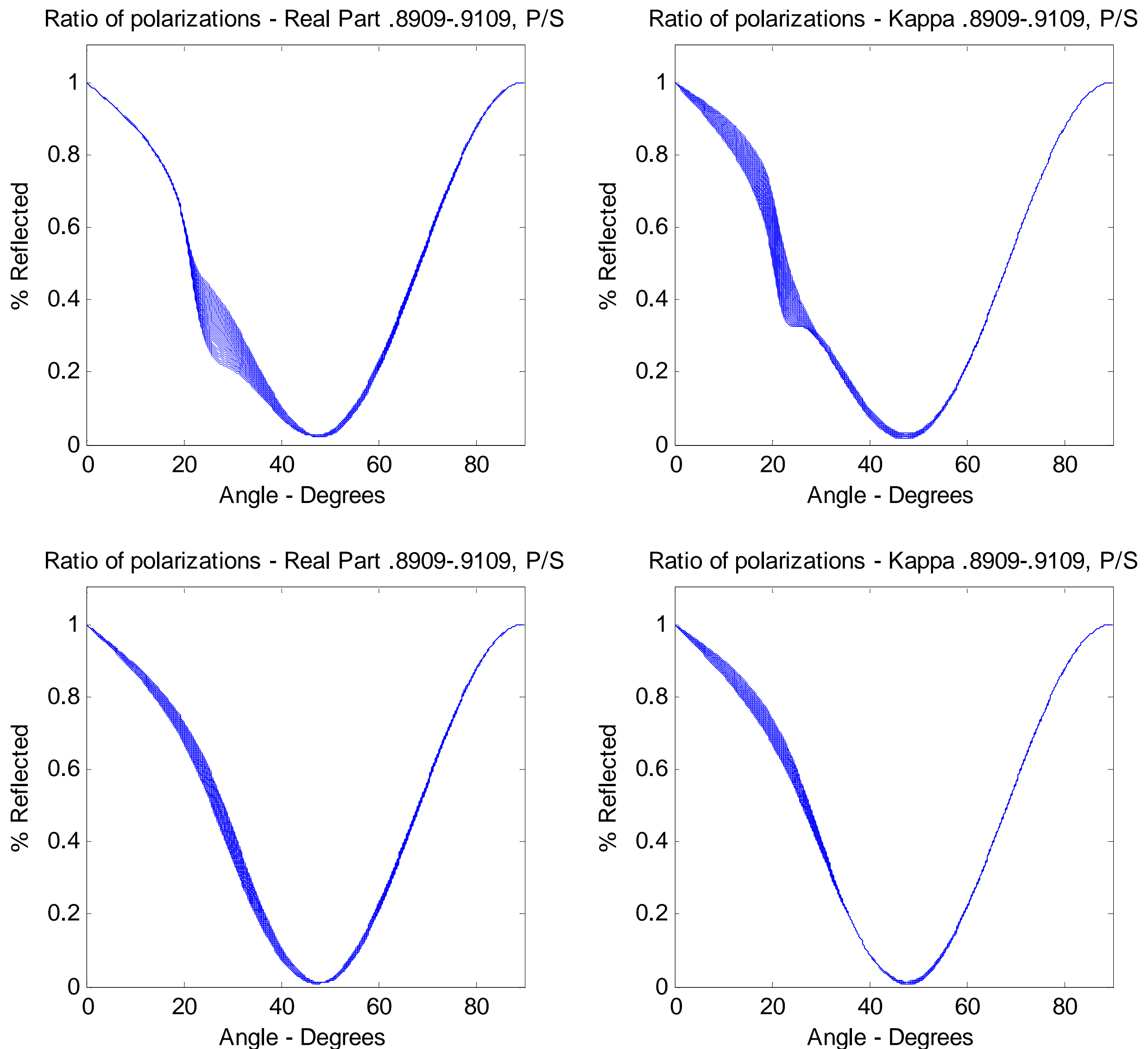

Figure 3.2 – Curves of varying index of refraction generated in Matlab using a wavelength of 29.6 nm and thickness of 5 nm (The top two graphs) and 40 nm (The bottom two graphs), centered around the index of refraction N=.9109+i*.0853 (Index given by the Center for X-Ray Optics [9]).

3.2 Preparation and Procedures

Before taking measurements, there are preparation steps and procedures that are performed to ensure accuracy. The main preparatory step is to warm up the laser, allowing it to stabilize for about an hour will produce a brighter more stable beam, allowing more accurate and continuous measurements. After the laser is warmed up there are laser alignment procedures developed by graduate student N. Brimhall that are followed, and explained as follows: (depicted in figure 3.3)

1. At low power, align the infrared laser with apertures 1 and 2.

2. Move the sample to 90 degrees and adjust the sample angle until it reflects the laser beam back through the apertures. A HeNe laser, a simple red laser, can also be used temporarily in place of the infrared laser system.

3. Turn on the switch motor that inserts the HeNe mirror into the laser path. Align the HeNe laser along the same path as the infrared laser, adjust until the beams reflect back from the sample.

4. Move the sample out of the laser path with the linear motor.

5. To align the detector, adjust the detector angle until the HeNe laser is centered on the grating.

6. Move the sample back into the beam. Because the sample motor is on top of the detector motor, moving the detector motor also moves the sample. Adjust the sample angle again so that it is reflecting the HeNe laser back along the same path (90 degrees).

7. Move the sample angle to 0 degrees. Align the sample position by adjusting the micrometer on the sample stage until the sample is cutting off half of the HeNe beam.

8. The vacuum gauge on the secondary vacuum chamber causes a physical constraint such that the MCP arm cannot be moved to 0 degrees at the same time that the detector arm is moved to 0 degrees. To align the MCP arm, move the detector angle to any angle greater than 10 degrees. Move the MCP arm angle to 0 degrees and adjust until the legs line up.

9. To align the grating angle, move the sample angle to half of what the detector angle is. This reflects the HeNe laser onto the grating. Move the grating angle to 0 degrees and adjust this angle until the grating is cutting off half of the HeNe beam.

10. The grating and MCP arm angles are now both at 0 degrees. To see harmonics, the grating should be moved to approximately 8 degrees and the MCP arm should be moved to approximately 19 degrees. These angles can be adjusted while viewing harmonics to view desired harmonic orders.

11. To prepare the positioning system for an incident intensity measurement, which is usually the first step in a reflectance scan, move the detector angle to 0 degrees, the sample angle to 90 degrees, and move the sample out of the beam with the linear sample stage.

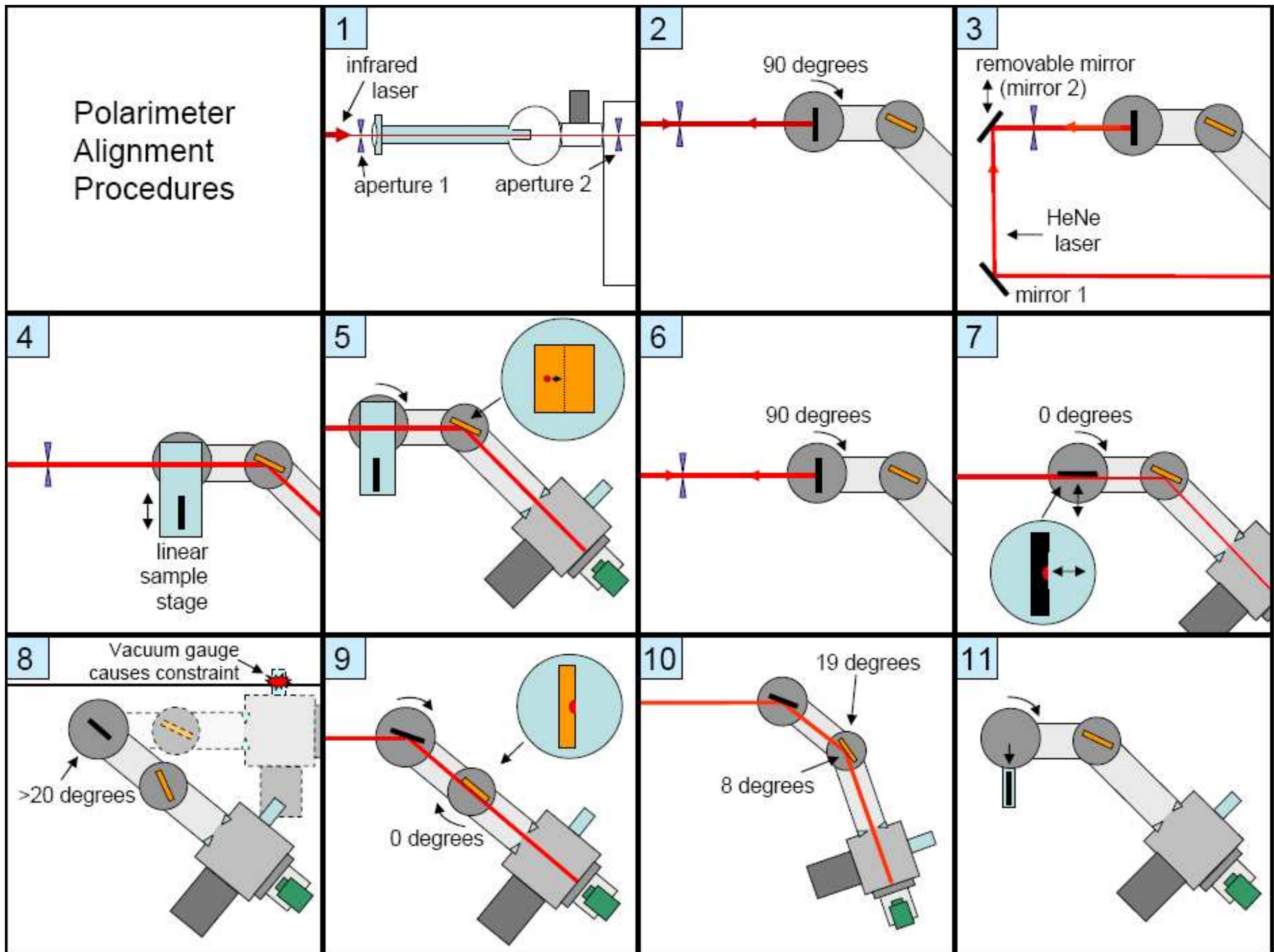

Figure 3.3 – The procedural steps for aligning the Polarimeter [3]

After the equipment is properly aligned, the molybdenum foil is set in place and the vacuum pumps are turned on to evacuate the air in the chambers. After the pressure in the chambers reaches their respective minimums, the first chamber is filled to the desired pressure of the chosen gas. S and p polarized light is measured individually without the sample in place, using only the grating to separate the harmonics, as an incident beam measurement. The incident measurement is used to calculate total reflectance percentages, and to remove the effect that the grating will have on the rest of the measurements. The sample is moved into place to begin taking measurements, starting at 5 degrees off

grazing, a measurement of the s polarization is taken then by turning the polarizer a measurement of the p polarization is taken. This is then repeated seven more times before moving to the next angle, making eight measurements of each polarization. These eight measurements are averaged together to give cleaner and more accurate data points. After getting data for 5 degrees, the angle is increased by increments of 2.5 until the p polarization is too dim to measure, being subject to Brewster's angle.

3.3 Reflection of EUV

3.3.1 *Sample Material*

Since the main part of this experiment is to test the accuracy of the equipment and capability of determining the index of refraction for EUV wavelengths, a material with a known index of refraction for these wavelengths has been chosen as a test. The sample being used is a thin layer of silicon-dioxide on a silicon base, the index for which can be obtained from the Center for X-Ray Optics (CXRO). During the mathematical modeling, the value used for this material was the value given by CXRO at a specified wavelength. For the graphs in figures 3.1 and 3.1 the wavelength used was 29.6 nm, which would be the 27th harmonic order, and the corresponding index of refraction giving by CXRO for this wavelength is N=.9109+i*.0853. [9] For these wavelengths the shift in the index of refraction from one harmonic order to another is more noticeable than when using visible light (400-700 nm), and for the comparisons against the accepted value of index of refraction would be different for every harmonic.

3.3.2 *Sample Thickness*

In the process of observing the variations in the data curves of the computer model, it was determined that the original sample of ~27 nm, was essentially infinitely thick when reflecting EUV. The model also showed that the variation in the data curve would be most observable for sample

thicknesses of 16 nm or less. These variations in the data curve would lower the error in calculation of the index of refraction from experimental data, whereas if the curve shifted very slightly the calculated index may be right, but the error would be larger. Another sample of silicon-dioxide was used, with the layer only 2 nm thick, instead of the original 27 nm.

3.4 Analyzing Data

After gathering all the data, the intensity of the separate harmonic orders was used to determine the reflectance percentage at each of the angles and incident for s and p. A ratio of the two polarizations was then taken to obtain a value for R_p/R_s where R_p is the reflectance of the p-polarized light, and R_s is the reflectance of the s-polarization. Before making a plot and fitting a graph, all the data points were divided by the incidents ratio of p/s to remove the effects of the grating, leaving only the reflectance off of the sample. A plot constructed out of the data points is shown in figure 3.3.

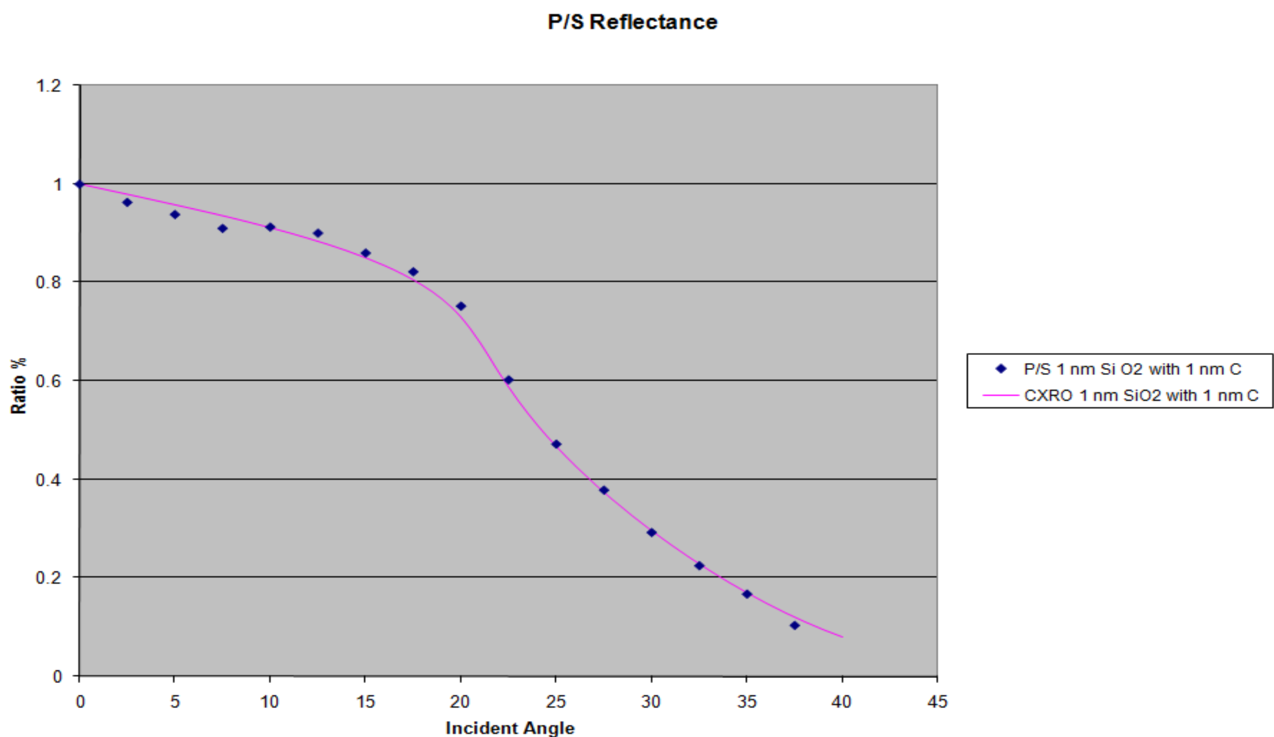

Figure 3.4 – data for R_p/R_s measurements off the 2 nm sample, compared with CXRO

The constants for silicon dioxide are available at the CXRO website. The values we obtained for the ratio of reflectance can then be compared with the modeled curve of the same ratio created by using the data obtained from CXRO, as depicted in figures 3.4, 3.5, and 3.6. Figure 3.4 is one of the data curves we made for the 2 nm sample, and from the actual measurements we determined that the silicon dioxide layer is only 1 nm with a 1 nm layer contamination of carbon. This layer of contamination of carbon was also present on the 27 nm sample. Although our samples could be cleaned using an ozone lamp, it would be nearly an hour before we are able to get it into a vacuum, allowing plenty of time for a new layer of contamination to form.

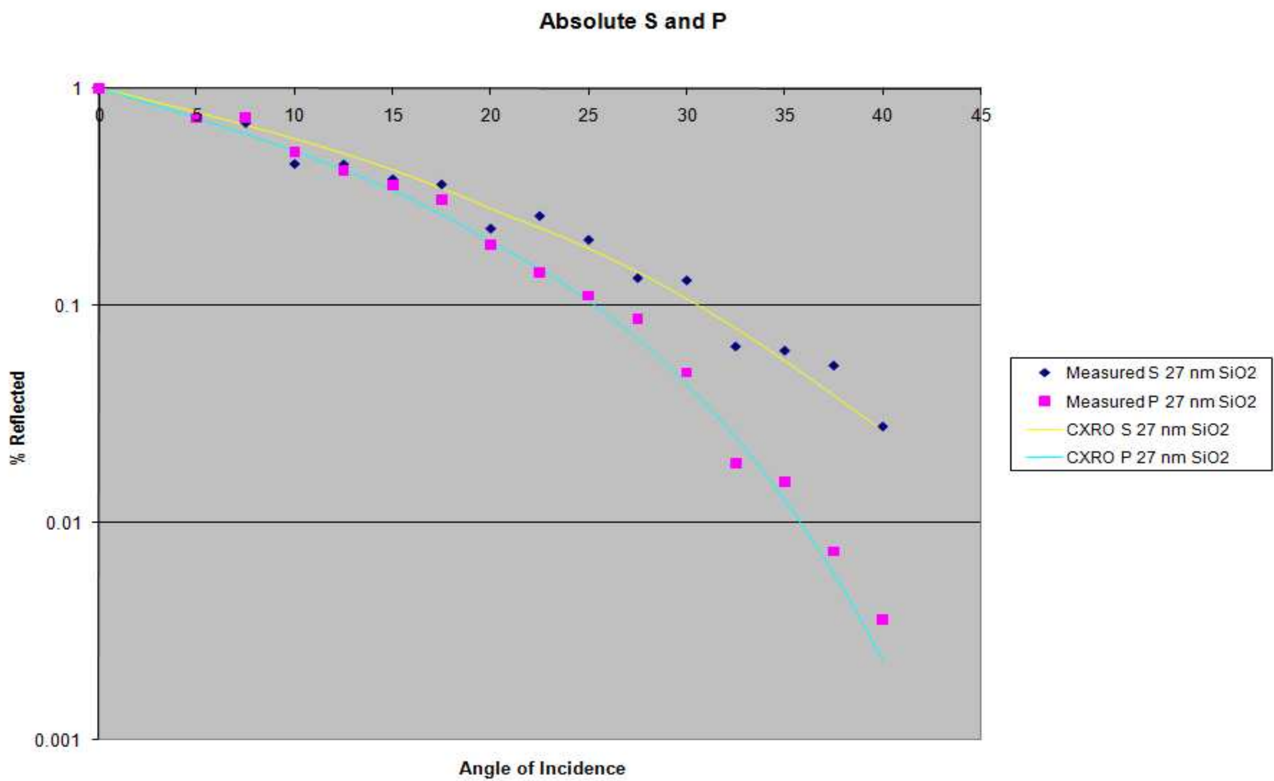

Figure 3.5 – data for Absolute R_p and R_s measurements, compared with measurements from CXRO

As depicted in figure 3.5, the ability to choose the polarization of our EUV beam gives us two different sets of data, the values for the absolute reflectance of the p and s polarizations separately. Although this ability to choose polarization is an advantage, this system has more noise in the

measurements than other sources; we take the ratio of the polarizations to sacrifice our advantage for more accuracy, as demonstrated with figure 3.6. The variance of our data points dropped considerably when the ratio is taken.

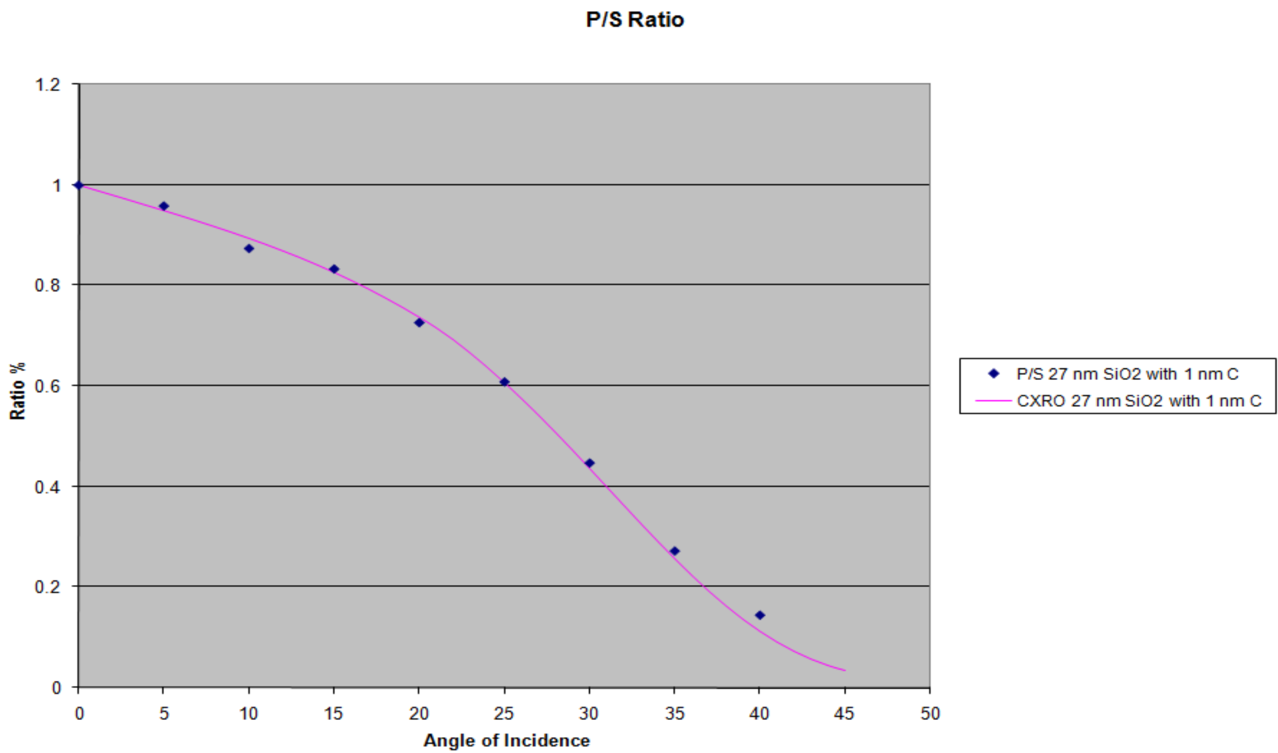

Figure 3.6 – data for R_p/R_s measurements off the 27 nm sample, compared with CXRO

Figures 3.4 and 3.6 also depict the change of the data curve from using a different sample thickness. When attempting to calculate the thickness of the 27 nm sample using a least-squares fitting method, it would always return the input value without changing it. But when calculating the thickness of the thinner sample least-squares fitting had very little trouble in determining how thick it is.

CHAPTER 4 CONCLUSION

4.1 Conclusion

The measurements made by the polarimeter at BYU were able to fit the reflectance curve provided by CXRO for silicon-dioxide on a silicon substrate. This fitted curve has an error within expected ranges, and has more accuracy with the ratio of the polarized beams as opposed to the curve measured separately. The polarimeter at BYU is capable of gathering measurements accurate enough to calculate the index of refraction and thickness (If under 17 nm) for a chosen material.

4.2 Ideas for New Study

After concluding this stage of the research Professor Peatross, the head of this research, has proposed new ideas to improve the accuracy of the measurements. Now that we have determined that a very thin sample would be more effective in measuring, one proposed plan is to insert an apparatus for thin film deposition inside of the chamber, which would not allow time for the sample to become contaminated before measuring. This apparatus would apply a thin layer of a chosen material which would then immediately be used in the reflectance measurements to determine not only the index of refraction but also the thickness of the layer deposited. Another proposed idea is to install an ozone lamp in the chamber that will clean the sample immediately before pumping out the air (and ozone). The vacuum pump would then need an exhaust house attached to keep the ozone from being vented into the lab.

REFERENCES

[1] “ALS Quick Facts,” http://www-als.lbl.gov/als/aboutals/alsquickfacts.html (Accessed February 28, 2009)

[2] Bakshi, Vivek. (2008). *EUV Lithography*. John Wiley & Sons Inc.

[3] Brimhall, N. Extreme Ultraviolet Polarimetry with Laser-Generated High-Order Harmonics, (Masters, Brigham Young University).

[4] Fitzgerald, R. (2000). “Pulse shaping improves efficiency of soft X-ray harmonic generation.” *Physics Today*, 24-28.

[5] Imazono, T; Ishino, M; Koike, M; Kimura, H; Hirono, T; Sano, K. “Performance of a reflection-type polarizer by use of muscovite mica crystal in the soft x-ray region of 1 keV.” *Review of Scientific Instruments*, Volume 76, Issue 2, pp. 023104-023104-4 (2005)

[6] “MATLAB - The Language of Technical Computing.” http://www.mathworks.com/products/matlab/ (Accessed February 28, 2009)

[7] Peatross, J., & Ware, M. (2008). *Physics of light and optics*. Provo, UT: Brigham Young University.

[8] “What are the uses and hazards of waves that form the Electromagnetic Spectrum?” http://www.antonine-education.co.uk/index.htm (Accessed October 7, 2008).

[9] “X-ray optics tools.” http://www-cxro.lbl.gov/index.php?content=/tools.html (Accessed October 7, 2008).

Appendix: Matlab Code

```
%Matlab Program to model the reflectance off of a thin layer using
%     matrix equations.
%Nathan Heilmann, 2008

function matsurf
clear all;
%% This section of subplot is to refresh the subplots without closing them.
y=5;
subplot(2,3,1,'replace');  plot(y);
subplot(2,3,2,'replace');  plot(y);
subplot(2,3,3,'replace');  plot(y);
subplot(2,3,4,'replace');  plot(y);
subplot(2,3,5,'replace');  plot(y);
subplot(2,3,6,'replace');  plot(y);
%End point of new graphing code.

%% Constants of the Thin Layers, subtrate, and the incident beam
%The index of refraction for the layer(s)
N1=.9167+i*.02357; %C
N2=.9109+i*.0853; %SiO2 .9485+i*.03137
%The index of refraction for the substrate
Ns=.9333+i*.0087; %Si
%The thicknesses of the subsequint layers
d1=0;
d2=4;
%The wavelength
wavelength=29.6;

%% Calculations for the Reflectance
%z-v is the number of steps the program takes, see alterations below
z=41;
v=1;
while v<z

    for th=.00001:pi/1000:pi/2;
        Si=sin(th);          Ci=cos(th);
        S1=Si/N1;            C1=sqrt(1-S1^2);
        S2=Si/N2;            C2=sqrt(1-S2^2);
        St=Si/Ns;            Ct=sqrt(1-St^2);

        k1=2*pi*N1/wavelength;
        B1=k1*d1*C1;
        k2=2*pi*N2/wavelength;
        B2=k2*d2*C2;

        Ms1=[cos(B1),-i*sin(B1)/(N1*C1);-i*N1*C1*sin(B1),cos(B1)];
        Ms2=[cos(B2),-i*sin(B2)/(N2*C2);-i*N2*C2*sin(B2),cos(B2)];
        Mp1=[cos(B1),-i*sin(B1)*C1/N1;-i*N1*sin(B1)/C1,cos(B1)];
        Mp2=[cos(B2),-i*sin(B2)*C2/N2;-i*N2*sin(B2)/C2,cos(B2)];

        As=(1/(2*Ci))*[Ci,1;Ci,-1]*Ms1*Ms2*[1,0;Ns*Ct,0];
        Ap=(1/(2*Ci))*[1,Ci;1,-Ci]*Mp1*Mp2*[Ct,0;Ns,0];
```

```
        n=round(1+th/(pi/1000));
        theta(n)=th;
        rs(n)=As(2,1)/As(1,1);
        rp(n)=Ap(2,1)/Ap(1,1);
    end

Rs=abs(rs).^2;
Rp=abs(rp).^2;
ratio=Rp./Rs;

%% These are the alterations to take place
v=v+1;
%N1=N1+.001+i*.001;
N2=N2+i*.00025;
%Ns=Ns+.001+i*.0001;
%d1=d1+.01;
%d2=d2+.1;
%wavelength=wavelength-.1;

%% Plotting The Data
d=90-theta*180/pi;
subplot(2,3,1)
plot(d,Rs,'b'); axis([0 40 0 1.1]); hold on
title('Reflection of S-polarization')
subplot(2,3,2)
plot(d,Rp,'b'); axis([0 40 0 1.1]); hold on
title('Reflection of P-polarization')
subplot(2,3,3)
plot(d,ratio,'b'); axis([0 40 0 1.1]); hold on
title('Ratio of polarizations, P/S')
subplot(2,3,4)
semilogy(d,Rs,'b'); axis([0 40 0 1.1]); hold on
title('Logrithmic Plot of S-polarization')
subplot(2,3,5)
semilogy(d,Rp,'b'); axis([0 40 0 1.1]); hold on
title('Logrithmic Plot of P-polarization')
subplot(2,3,6)
semilogy(d,Rs,'b'); axis([0 40 0 1.1]); hold on;  semilogy(d,Rp,'g')
title('Logrithmic, Blue-S, Green-P')
drawnow
end

%% These make the red line that shows where the plotting ends.
subplot(2,3,1);   plot(d,Rs,'r');
subplot(2,3,2);   plot(d,Rp,'r');
subplot(2,3,3);   plot(d,ratio,'r');
subplot(2,3,4);   semilogy(d,Rs,'r');
subplot(2,3,5);   semilogy(d,Rp,'r');
subplot(2,3,6);   semilogy(d,Rs,'r');   semilogy(d,Rp,'r')
%This is the end of the red line code.
hold off
```